Rapid #: -10193471

CROSS REF ID: **1289493**

LENDER: **PUL :: Interlibrary Services, Firestone**

BORROWER: **WAU :: Suzzallo Library**

TYPE:	Article CC:CCG
JOURNAL TITLE:	Geophysical monograph
USER JOURNAL TITLE:	Geophysical Monograph,Geophysical monograph.,
ARTICLE TITLE:	Galapagos magma chambers
ARTICLE AUTHOR:	Geist, Dennis J.
VOLUME:	204
ISSUE:	
MONTH:	
YEAR:	2014
PAGES:	,55-,,-
ISSN:	0065-8448
OCLC #:	

Processed by RapidX: 2/7/2016 3:08:40 PM

5

Galápagos Magma Chambers

Dennis J. Geist[1], George Bergantz[2], and William W. Chadwick, Jr.[3]

ABSTRACT

Each of the seven shield volcanoes of the western Galápagos has a large caldera—direct evidence of shallow magma chambers. The volcanoes are of three petrologic types: (1) Diverse volcanoes that erupt more primitive magmas; (2) monotonic volcanoes that erupt evolved tholeiites and are very active; and (3) dying volcanoes that erupt infrequently and produce siliceous magmas. Deformation measurements indicate that the magma chambers of the monotonic volcanoes are flat-topped and reside less than 2 km below the caldera floor. The magma chambers of the diverse volcanoes are deeper and ephemeral. Trace element heterogeneity of melt inclusions and lavas that erupted over the course of a few centuries indicates the absence of a large, homogeneous, largely liquid magma reservoir at the monotonous volcanoes. A three-stage evolutionary model for Galápagos magma chambers is proposed. At the leading edge of the hotspot, magmas are only partly buffered thermally and chemically. They evolve by cooling and crystallization of olivine, pyroxene, and plagioclase throughout the lithosphere. The crystals form a growing mush pile. Once a volcano becomes mature, magmas transit through the mush pile before residing in a shallow subcaldera sill, which buffers all magmas thermally and chemically and creates a monotonous suite. Buoyant plagioclase accumulates at the top of the shallow sill and olivine gabbro mush forms at its base. Magmas erode the mush as they are transported from the shallow sill to both summit and flank vents. In the dying phase, which occurs when the volcano is carried away from the hotspot, the mush cools, begins to solidify, and silicic magma is generated.

5.1. INTRODUCTION

The lack of direct observations of active magma chambers has led to a wide variety of conceptual models for their physical state, especially gradients in temperature, crystallinity, and liquid compositions. The various concepts are based on constraints from forensic studies of plutons, inferences from study of eruptive rocks, and geophysical measurements, none of which provide definitive evidence for the state of magma in crustal reservoirs. A large body of theoretical work based on analogue and computational models of solidifying systems, multiphase flow, and fluid dynamics have also proposed a number of disparate concepts of magma chamber processes, but many of these are limited by a lack of observational tests guided by natural systems.

Differences between conceptual models of magma chambers are largely based on the distribution of crystals and liquids in the chamber as a function of time. For example, *McBirney* [1981] and *Huppert and Sparks* [1988] visualize a largely liquid magma body surrounded by a narrow boundary layer with strong gradients in temperature, crystallinity, and composition. *Marsh* [1989] pointed out the importance of advancing solidification fronts—rheologic boundaries that migrate inward from the margins of the chamber in which most of the macro-scale

[1] *Department of Geological Sciences, University of Idaho*
[2] *Department of Earth and Space Sciences, University of Washington*
[3] *Hatfield Marine Science Center, Oregon State University*

The Galápagos: A Natural Laboratory for the Earth Sciences, Geophysical Monograph 204. First Edition.
Edited by Karen S. Harpp, Eric Mittelstaedt, Noémi d'Ozouville, and David W. Graham.

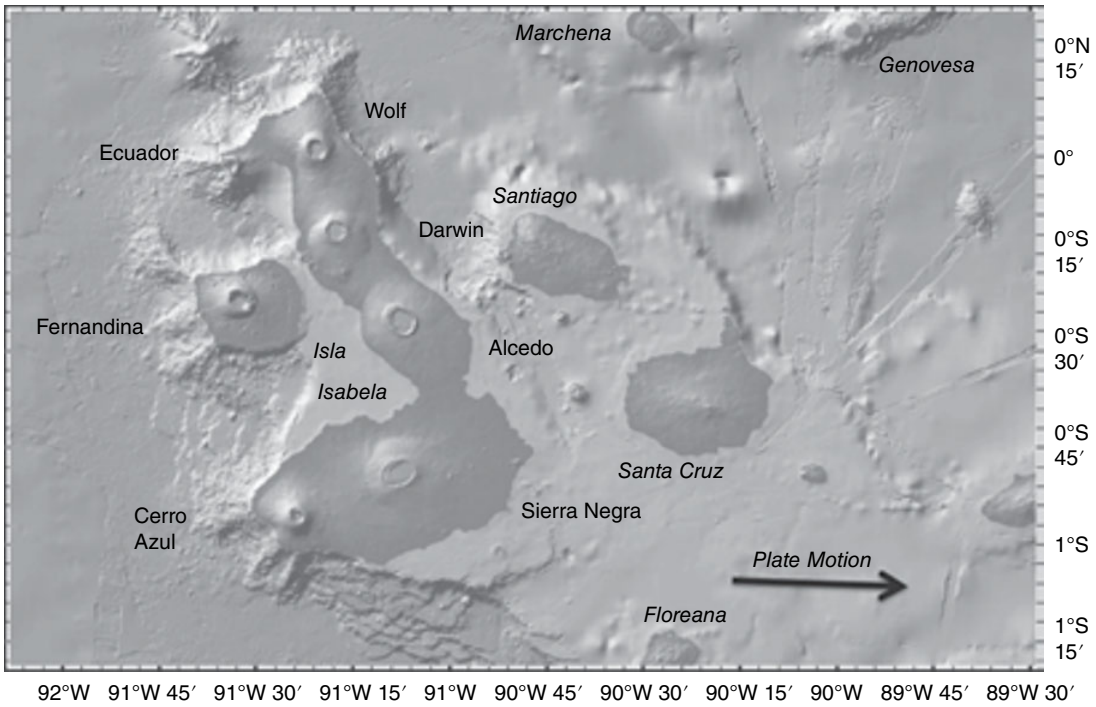

Figure 5.1 Shaded relief map of the Galápagos Platform and the western Galápagos Islands (four other islands lie outside the map area).

differentiation takes place. More recently, petrologists and geophysicists have emphasized systems with broad crystallinity gradients in both mafic and siliceous chambers, where liquid-dominated bodies overlie, or are interlayered with, large volumes of crystalline mushes [*Sinton and Detrick*, 1992; *Kelemen et al*., 1997; *Bachmann and Bergantz*, 2004]. A major conceptual breakthrough of more recent work has been the recognition that crystal-rich magma (mush, which is magma with 25–55% crystals) [*Marsh*, 1989] could constitute the dominant volume of magma chambers, but this magma is rarely sampled by eruptions [*Bergantz*, 1995; *Marsh*, 2005].

Studies of the polygenetic shield volcanoes of the western Galápagos (Figure 5.1) provide insight into the evolution of their magma chambers and offer several advantages to other systems. First, we know that shallow magma chambers exist because of the large calderas that typify these volcanoes. Second, Galápagos shield volcanoes are overwhelmingly basaltic and lie on young, thin basaltic ocean crust. Thus, they are relatively simple systems dominated by crystallization of plagioclase, olivine, and clinopyroxene, in which assimilation is negligible [*Geist et al*., 1998]. Third, they are among the most rapidly deforming volcanoes on Earth, and inter-eruption inflation reveals aspects of the geometry and the timing of the filling of shallow magma bodies that are not available elsewhere. Fourth, because the submarine sectors of several of the volcanoes are now well-studied, the entire growth history of the volcanoes is revealed, and nearly 5 km of vertical relief through the eruptive section is exposed. Fifth, the seven active shields allow for comparison and contrast of magmatic systems in different settings, from birth on the abyssal seafloor to the waning stages as a volcano is carried away from the focus of the Galápagos hotspot.

5.2. EVIDENCE FROM VOLCANIC HISTORY AND GEOMORPHOLOGY

The Galápagos Islands are a hotspot-related chain that lies adjacent to the Galápagos Spreading Center (GSC). The islands lie on the Nazca plate, which moves almost directly east at about 51 km/my (no-net rotation reference frame) [*Argus et al.,* 2010]. Consequently, the youngest volcanoes lie in the western part of the archipelago, and the seven shield volcanoes of Isabela and Fernandina are the focus of this paper (Figure 5.1).

Sixty-two eruptions have been observed and recorded in the western Galápagos, the first in 1797 [*Simkin and Siebert*, 1994]. The actual number of eruptions is likely to be nearly twice this number, however, as twenty-six eruptions have been witnessed since 1950 (when the islands were permanently inhabited), suggesting that prior eruptions were likely underreported (Figure 5.2). There is a pattern to the activity: Fernandina, Wolf, Cerro Azul, and Sierra Negra have each had more than ten recorded eruptions, whereas Alcedo, Darwin, and Ecuador have

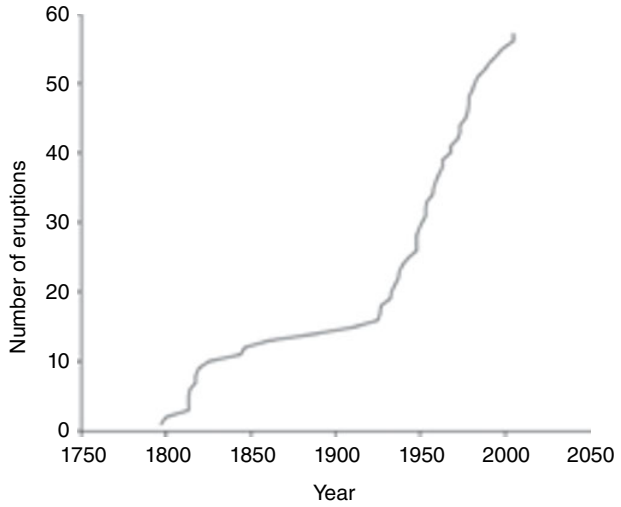

Figure 5.2 Cumulative number of eruptions reported from the western Galápagos. Human inhabitation and visitation increased dramatically in the mid-20th century. The eruption rate since 1950 has been approximately one eruption every two years.

had only one or no observed eruptions. Alcedo and Darwin have both been carried away from the core of the Galápagos hotspot, and thus may be in a dying phase of evolution. In contrast, Ecuador is at the leading edge, lying west of Volcan Wolf, but it has undergone a sector collapse, which may have affected its recent eruption rate [*Geist et al*., 2002].

The western Galápagos shields have characteristic morphologies, which in part reflect their shallow magmatic plumbing systems. In addition to their large and deep calderas, they have unusually steep upper slopes and circumferential eruptive fissures on their upper parts, and radial fissures on their lower flanks [*McBirney and Williams*, 1969; *Nordlie*, 1973; *Mouginis-Mark et al*., 1996; *Chadwick and Howard*, 1991]. The distribution of vents is believed to result from a combination of stresses imparted by a shallow magma chamber, surface loading, and the steep slopes and caldera walls [*Chadwick and Dieterich*, 1995; *Reynolds et al*., 1995; *Chadwick et al*., 2011]. The steep summit carapace forms because low-volume, stubby lava flows erupt from the circumferential fissures, and more voluminous lava flows erupt from the lower radial vents [*Simkin*, 1972; *Naumann and Geist*, 2000]. Both circumferential and radial eruptive vents have fed historical eruptions in about equal numbers, and mechanical modeling suggests that they may alternate in time on a given volcano in a stress feedback relationship. Circumferential dikes are fed from the upper margins of flat-topped subcaldera sill-like magma reservoirs [*Chadwick and Dieterich*, 1995; *Yun et al*., 2006; *Chadwick et al*., 2011]. Because radial dikes feed lower-elevation and submarine eruptions, they likely originate from a deeper part of the system.

The submarine flanks of the volcanoes differ substantially from their subaerial parts: focused rift zones characterize the submarine parts of Fernandina, Cerro Azul, Ecuador, and Wolf volcanoes [*Geist et al*., 2006b; 2008a], whereas the subaerial volcanoes only have diffuse concentrations of radial vents in certain sectors [*Chadwick and Howard*, 1991]. The greater degree of focusing of the vents on the submarine slopes is attributed to a positive feedback between topography stubby lavas, and dike emplacement [*Geist et al*., 2006b].

The Galápagos calderas are up to hundreds of meters deep, but evidence suggests they do not form by singular collapse events tied to individual voluminous eruptions. Instead, the calderas appear to form incrementally by repeated small co-eruption collapse events, sometimes in response to remarkably small eruptions. Wolf, Cerro Azul, Alcedo, and Fernandina each have undergone several cycles of partial refilling, followed by renewed collapse off-center from the previous collapses, exposing caldera-filling lavas in the new caldera wall [*Simkin and Howard*, 1970; *Chadwick et al*., 1991; *Rowland and Munro*, 1992; *Munro et al*., 1996; *Geist et al.,* 2005; *Naumann and Geist,* 2000; *Geist et al.,* 1994; *Allan and Simkin*, 2000; *Howard*, 2010]. Sierra Negra, Alcedo, and Darwin volcanoes are currently in a phase of caldera filling [*Geist et al*., 1994; *Reynolds and Geist*, 1995; *Naumann and Geist*, 2000]. No overt change in the magmas' compositions can be tied to caldera filling versus caldera subsidence, so foundering versus filling is probably not simply tied to magma supply rate.

One of the largest caldera collapses in historical times took place at Fernandina in 1968, when the caldera collapsed 350 m over a period of twelve days, accounting for a volume of 1.5 km^3 [*Simkin and Howard*, 1970; *Filson et al*., 1973; *Howard*, 2010]; the volume of erupted material accompanying this event was less than 1% of the volume of the caldera collapse. Either a major submarine eruption went undetected (at the same time as the small subaerial eruption), a large intrusion moved a significant volume of magma from the sub-caldera magma reservoir into the volcano flanks (but did not erupt), or the caldera collapse was driven by loading of the crust with dense, intrusive rocks [*Walker*, 1988].

5.3. EVIDENCE FROM DEFORMATION AND GRAVITY

The earliest measurements of ground deformation in Galápagos with satellite radar interferometry (InSAR) found that intrusion of magma into the shallow crust was occurring at six of the seven western volcanoes, as evidenced by uplift of their caldera floors, Ecuador being the

lone exception [*Amelung et al*., 2000]. The magnitude and distribution of observed ground deformation enable estimates of the depths, shapes, and volume changes of the magma bodies that underlie the calderas. Model inversions suggest that flat-topped chambers exist at each of the volcanoes (although the geometry of most are poorly constrained), ranging in depth from 1–3 km except for Cerro Azul, which has a deeper chamber (5 km). Fernandina appears to have both a shallow, sill-like magma body at approximately 1 km and a deeper reservoir of unknown shape at approximately 5 km [*Geist et al*., 2006a; *Chadwick et al*., 2011; *Bagnardi and Amelung*, 2012]. The dimensions of the tops of the shallow magma bodies are relatively well-constrained by deformation measurements, but their deeper geometry is uncertain [*Yun et al*., 2006].

Deformation at Sierra Negra is the best-characterized of all of the Galápagos volcanoes because of its remarkable rates of inflation, monitoring by both InSAR [*Amelung et al*., 2000; *Jónsson et al*., 2005; *Yun et al*., 2006] and a continuous GPS network [*Geist et al*., 2006a; *Chadwick et al*., 2006; *Geist et al*., 2008b], and field mapping of intra-caldera faults caused by magmatically induced inflation [*Reynolds et al*., 1995; *Jónsson et al*., 2005; *Jónsson*, 2009]. Inverse models provide estimates of the depth to the top of the magma body ranging from 1.9–2.1 km below the caldera floor [*Amelung et al*., 2000; *Yun et al*., 2006; *Geist et al*., 2006a; *Chadwick et al*., 2006]. The ratio of horizontal to vertical deformation indicates that the magma body has a flat roof, like a sill, a shape that fits the data better than a spherical source. Modeled sills have plan dimensions smaller than the caldera by about 1 km [*Amelung et a*l., 2000; *Geist et al*., 2006a; *Yun et al*., 2006; *Chadwick et al*., 2006].

A deformation record from the last twenty years now exists at Sierra Negra, including the periods both before and after the 2005 eruption. The data reveal how the rates of inflation and deflation have varied with time, which in turn reflect the rate of intrusion into the shallow magma body (Figure 5.3). From 1992 to the 2005 eruption, the magma reservoir filled and became pressurized, although at a non-linear rate, including an episode of slight depressurization from 2000–2002 followed by accelerating uplift leading up to the eruption [*Chadwick et al*., 2006]. In 1998 and four times in 2004–2005, the roof of the chamber failed by trapdoor faulting of the caldera floor, resulting in M4-5.5 earthquakes with fault slip of nearly a meter [*Amelung et al*., 2000; *Jónsson et al*., 2005; *Chadwick et al*., 2006; *Jónsson*, 2009]. None of the pre-eruption earthquakes seemed to have much effect on the rate of inflation, except for the last and largest one that occurred just three hours before and was clearly associated with the onset of the 2005 eruption [*Chadwick et al*., 2006; *Yun et al*., 2006; *Geist et al*., 2008b].

Following nearly 5 m of deflation that accompanied the 2005 eruption, Sierra Negra began inflating immediately

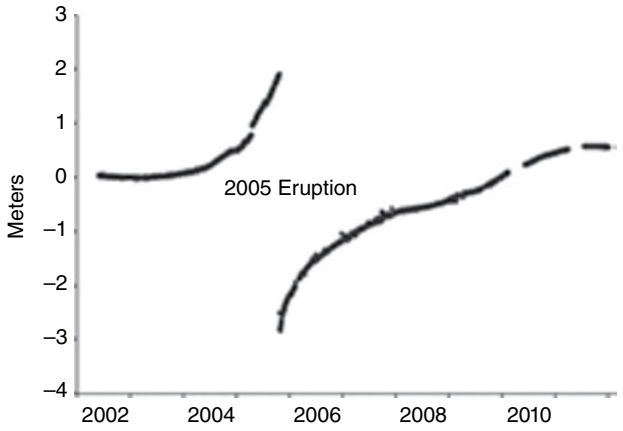

Figure 5.3 Time-series of continuous GPS data showing the vertical displacement of the floor of Sierra Negra's caldera for the period from 2002–2012 [data from *Geist et al*., 2006a, *Chadwick et al*., 2006, and unpublished data, Geist].

afterward [*Geist et al*., 2008b]. The inflation rate was initially high and gradually decreased for several years after the eruption, which we attribute to a steadily decreasing pressure gradient between the shallow reservoir and its deeper magma source, owing to repressurization of the shallow reservoir. Another possibility for the decreasing rate of inflation since 2005 is the deformation of viscoelastic material surrounding the shallow magma chambers after rapid repressurization following the eruption. Several fluctuations over the past seven years are superimposed on this trend, and the volcano began another episode of slight deflation in late 2011. If we assume the magma reservoir at Sierra Negra is a sill of the dimensions modeled by *Geist et al*. [2006a], then the deformation since the 2005 eruption indicates that $62 \times 10^6\,m^3$ of magma has been added (at an average rate of $12 \times 10^6\,m^3/y$), roughly a third of the $150 \times 10^6\,m^3$ of lava erupted in 2005 [*Geist et al*., 2008b]. Although the rate of magma input into the shallow chamber has fluctuated more than two-fold and even stopped in 2011, the long-term supply to the magma chamber has been remarkably steady for years and is not characterized by high Reynolds number "episodic fountains," as some have visualized and modeled (Figure 5.3) [*Huppert et al*., 1986].

The 2005 eruption at Sierra Negra was accompanied by a 950 microgal decrease in the free-air corrected gravity [*Vigouroux et al*., 2008]. This is attributed to expansion of the magma body by vesiculation as the magmatic overpressure was reduced. Over the next two years the gravity anomaly reverted to near its original state, indicating that the edifice re-densified, either due to gas segregation and loss or pressurization and redissolution of the volatiles.

Fernandina volcano also erupted in 2005 and again in 2009. Modeling of deformation data from both InSAR and campaign-GPS associated with the 2005 eruption

reveals pre- and post-eruption inflation from a shallow sill at approximately 1 km depth beneath the caldera, and syn-eruptive deflation at approximately 5 km depth [*Chadwick et al.*, 2011]. This is attributed to a deep region of storage, which was pressurized prior to the eruption and which feeds the shallow reservoir. The same bi-level reservoir system is apparent from InSAR data before and after the 2009 eruption [*Bagnardi and Amelung*, 2012].

Fernandina and Sierra Negra's calderas are characterized by +20–30 mgal Bouguer anomalies (the only volcanoes where gravity has been measured) [*Ryland*, 1971; *Geist et al.*, 2006a; *Vigouroux et al.*, 2008]. The best explanation for this is that the subcaldera magma bodies are underlain by a volume of dense cumulates. A simple model of a vertical cylinder of mafic intrusive rocks (density 400 kg/m^3 greater than basalt) whose top is 2 km beneath the caldera floor, and with a radius of 5 km, would need to be approximately 5 km high to account for a +30 mgal anomaly.

5.4. EVIDENCE FROM MAGMA COMPOSITIONS AND CRYSTALS

Major and trace element variations indicate that the magmas at each volcano have undergone substantial fractionation of plagioclase, olivine, and augite, both in the deep crust and at shallow levels [*Geist et al.*, 1998). Alcedo volcano's dacite and rhyolite evolved by advanced crystallization also involving apatite, pigeonite, and titanomagnetite, a consequence of its magmas having cooled to less than 900 °C [*Geist et al.*, 1996]. The depth of multiphase saturation can be assessed by the pressure-sensitive positions of cotectics and invariant points [*Geist et al.*, 1998]. Magmas from Volcan Wolf, Fernandina, Alcedo, and Sierra Negra are multisaturated at mid- to shallow-crustal conditions. In contrast, many magmas from Cerro Azul and Volcan Ecuador erupted from deeper levels in the lower crust [*Geist et al.*, 1998; *Naumann et al.*, 2002]. Deep crustal xenoliths at Floreana volcano have compositions which indicate that they crystallized from magmas like those currently supplying the western volcanoes [*Lyons et al.*, 2007]. They show that shield-building Floreana magmas underwent some crystallization in the lower crust, although most crustal growth is from above, from shallow intrusions and lavas.

The compositional variation at each of the western shield volcanoes can be examined using kernel density estimation, which, unlike histograms, creates a smooth estimate of the population and does not require selection of bin end-points (Figure 5.4) [*Rudge*, 2008; *Wessa*, 2013]. Gaussian kernels were used, although these data sets do not have a strong dependence on the shape of the kernel. Smoothing bandwidth was selected by the "rule of thumb" method [*Rudge*, 2008] and was between 0.7 and 2.5 when analyzing Mg# (100*MgO/MgO + FeO*). The representative value

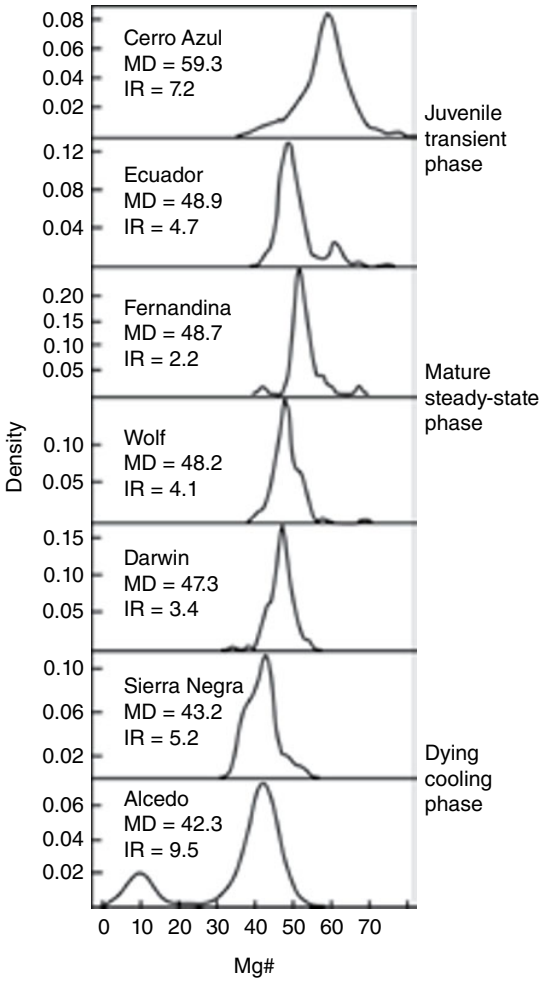

Figure 5.4 Probability density functions generated by kernel density estimation of Mg# for each of the seven western Galápagos shields [*Rudge*, 2008; *Wesse*, 2013]. MD stands for maximum density, and IR is inter-quartile range. All published analyses are used and thought to be representative of eruptive volume, except for Alcedo volcano. At Alcedo, the mapped volumes of siliceous and mafic rocks are used.

for each volcano is reported as the maximum density. The statistical dispersion is reported as inter-quartile range (IR), owing to the non-Gaussian distributions.

In basaltic magmas, the Mg# varies as a function of the amount of crystallization of mafic minerals (and is unaffected by plagioclase crystallization or accumulation), and hence provides a straightforward estimate of magmatic temperature. Calculations using the MELTS algorithm [*Ghiorso and Sack*, 1995] show that for primitive Galápagos magmas at 0.1 GPa (which are saturated with olivine + augite + plagioclase, with 0.5% H2O), Mg# drops one unit for every 3.6 °C of cooling. Although MgO is more closely correlated to temperature than Mg# in most suites, the latter is unaffected by the plagioclase accumulation, which demonstrably affects many whole-rock analyses.

The inter-quartile range (IR) of Mg# for all samples from Fernandina, Wolf, and Darwin volcanoes is less than 4.1, whereas for Sierra Negra, Cerro Azul, Ecuador, and Alcedo it is greater than 4.7 (Figure 5.4). We refer to the first set of volcanoes as compositionally "monotonous" and the second set as "diverse". The variation in Mg# of the monotonous volcanoes means that for their entire eruptive history (as preserved in surface exposures) the total magmatic temperature range is less than 30 °C. These remarkably small temperature differences are over time scales as long as 4,300 years at Fernandina [*Kurz et al.*, Chapter 4, this volume] and approximately 100,000 years at Wolf [*Geist et al.*, 2005]. The monotonous suites have been buffered thermally inside their magma chambers over millennial time scales, which limits their compositional diversity.

The diverse suites, in turn, are diverse because they erupt abnormally hot and cold magmas. Cerro Azul and Volcan Ecuador have erupted more MgO-rich lavas than the other volcanoes (Figure 5.4). Although some of the MgO-rich magmas have accumulated olivine, not all of them have done so [*Naumann et al.*, 2002; *Teasdale et al.*, 2005; *Geist et al.*, 2002]. Both of these volcanoes are at the western margin of the hotspot province. By contrast, Alcedo has erupted a complete tholeiitic series, including rhyolites, and some of Sierra Negra's magmas erupt at cooler temperatures and are saturated with titanomagnetite [*Geist et al.*, 1996]. Alcedo is "downstream" of Fernandina volcano and Sierra Negra is downstream of Cerro Azul (Figure 5.5). The 2 "hot" volcanoes are at the leading edge of the hotspot, and the 2 "cold" volcanoes with lowest Mg# are "downstream" of another volcano.

Galápagos lavas are erupted as a mixture of melt and phenocrysts, and the proportions of the mixtures change systematically as a function of the elevation of the eruptive vents. This relationship is most apparent on Fernandina, where the subaerial lavas contain up to 20% plagioclase but less than 4% mafic phenocrysts [*Allan and Simkin*, 2000], whereas the submarine lavas have up to 20% olivine phenocrysts [*Geist et al.*, 2006b]. Measurements of the compositions of olivine phenocrysts at Ecuador, Wolf, Cerro Azul, and Fernandina show that almost all are too magnesian to have crystallized from their host liquids [*Geist et al.*, 2002; 2005; 2006b; *Teasdale et al.*, 2005]. Instead, they crystallized from hotter, more magnesian magmas and were picked up by their host liquids a few hours to a few days before eruption [*Geist et al.*, 2006b]. Likewise, most of the erupted plagioclase phenocrysts are strongly out of equilibrium with their host liquids. Although a few glomerocrysts of several crystals are contained in many lavas, the vast majority of these exotic phenocrysts are discrete single crystals. This suggests the incorporation of a crystal mush, rather than assimilation of rocks.

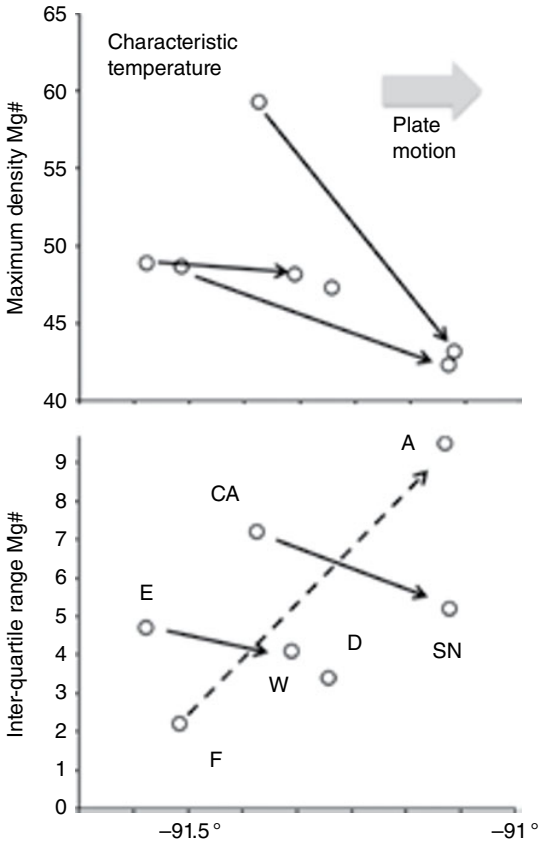

Figure 5.5 (Top) The statistical maximum density of the Mg# reflects the characteristic temperature of lavas erupted from each volcano. Longitude is meant to be a measure of the volcano's position relative to the focus of the magma supply at the core of the hotspot (to the west, or left, in this view). The "upstream" volcanoes—Fernandina (F), Ecuador (E), and Cerro Azul (CA)—erupt lavas of systematically higher temperature than their "downstream" complement: Alcedo (A), Wolf (W), and Sierra Negra (SN). (D indicates Darwin.) The arrows connect the complementary volcanoes. (Bottom) The statistical dispersion of compositions, and hence temperature variations, are different for the complementary pairs. Cerro Azul and Ecuador are in the early transient phase; therefore, compositional variability is lower at the complementary volcano, which is in the mature, steady-state phase. Fernandina is already in the mature phase, and its complement, Alcedo, is in the cooling, dying phase and erupts lavas of highly variable Mg#.

Although each of the western volcanoes is broadly homogeneous in terms of its trace element and isotopic ratios, precise analysis of age-constrained lavas at Ecuador and Wolf volcanoes reveal that there is measurable trace-element variation over millennial time scales. Moreover, melt inclusions hosted in olivine from Fernandina volcano reveal much greater compositional diversity than is represented by the lavas [*Hedfield*, 2003; *Kolesczar et al.*, 2009]. Conservative assumptions of the compositional variation of the input magmas, using

the melt inclusion data of *Kolesczar et al*. [2009], enable estimation of the residence time of magma within the shallow chambers [*Albarède*, 1993]. The residence time can be multiplied by the eruption rate to estimate the volume of the well-mixed chambers, and the results range from 0.10–0.18 km^3 [*Geist et al*., 2002; 2005]. If the magma bodies have horizontal dimensions comparable to those of the calderas (r = 3 km), then the chambers would be less than 100–700 m thick. In other words, they are at least eight times broader than they are thick, consistent with the sill-like geometries indicated by deformation modeling.

Fernandina, Wolf, Sierra Negra, and Cerro Azul volcanoes each have excesses of ^{230}Th, ^{226}Ra, and ^{210}Pb [*Handley et al*., 2011]. The ^{230}Th excesses are almost certainly due to melting processes, as supported by correlation of long-lived radiogenic isotopes and trace element ratios such as Nb/Zr. The relatively long half-life provides little information as to the residence time of magmas since melting. Although the mechanisms for generating ^{226}Ra and ^{210}Pb are not clear, it is thought that they are due to interaction between basaltic magmas and lithospheric rocks late in their ascent history, on a millennial to decadal time scale.

5.5. PETROLOGIC MONITORING OF ERUPTIONS

Improved communications and transportation have permitted immediate responses to several recent Galápagos eruptions, so samples have now been collected over the course of eruptions and related to eruptive order and the vigor and style of extrusion. Each of the eruptions has revealed new information on how Galápagos magmatic systems work. Time-series sampling of the 1998 eruption of Cerro Azul revealed that the lavas changed composition over the course of the eruption due to two processes [*Teasdale et al*., 2005]. During the first phase of the eruption, a new batch of magma mixed with magma that had resided in the east flank of the volcano since the previous eruption in 1979. During the second phase, the 1998 magma eroded and flushed a troctolitic (olivine + plagioclase ± augite) mush from deeper within the volcano.

In contrast, the 2005 eruption of Sierra Negra produced nearly aphyric tephra and lava, but the eruptive products were zoned, with slightly more evolved magma erupting first (approximately 20° cooler) [*Geist et al*., 2008b]. Otherwise, the compositions were homogeneous. It is proposed that the magma erupted from a shallow (about 2 km deep) sill, which had accumulated differentiated liquid near its upper margin.

Lavas from the 1995 and 2005 eruptions of Fernandina likewise preserve evidence of erosion of a crystal mush [*Chadwick et al*., 2011]. The 1995 eruption was from a radial fissure that extended from near the summit to the coast, and the lavas are choked with olivine + plagioclase phenocrysts that are interpreted to be an eroded mush. In contrast, the 2005 fissure was at the summit and circumferential, and its dike originated from the shallow subcaldera sill at approximately 1 km depth. The 2005 lavas contain little of the plagioclase + olivine debris found in the 1995 lavas [*Chadwick et al*., 2011].

5.6. SUMMARY OF INTERPRETATIONS

The geophysical, petrologic, and volcanologic data and interpretations cited above lead to the following synthetic model of Galápagos magma chambers.

- At all but Cerro Azul, the top of the magma chamber is flat, with horizontal dimensions slightly smaller than the diameter of the calderas (5–9 km). The top of the system is shallow, typically only about 1–3 km beneath the caldera. The shallow magma reservoir is no more that several hundred meters thick; therefore, it is a sill.
- Magmas evolve by crystallization at various depths in the crust, not just in the shallow sill. Deeper crustal crystallization is of dunite, wehrlite, and olivine gabbro. Currently, there is no constraint on the proportion of crystallization that occurs in the deep versus the shallow crust, but ongoing seismic studies may resolve this in the near future.
- Magmas within the "monotonous" volcanoes (Wolf, Fernandina, and Darwin) are thermochemically buffered; that is, they are of a steady-state composition, having undergone nearly identical amounts of cooling and crystallization for 10^3 to 10^5 years.
- There are two types of compositionally variable volcanoes. At the western margin of the hotspot, Ecuador and Cerro Azul erupt lavas that are hotter and compositionally more primitive than the steady-state compositions of the monotonous volcanoes. In contrast, the magmatic plumbing systems of Sierra Negra and Alcedo volcanoes, which are downstream of the hotspot, are cooling.
- Most "phenocrysts" did not crystallize from the groundmass that hosts them: they are extraneous cargo. The eroded material is crystal mush, not rocks. The subcaldera sill filters out most olivine and augite from magma that is eventually erupted on the subaerial slopes, except for plagioclase. Circumferential eruptions apparently tap this shallow part of the system. Mush consisting of olivine + plagioclase + augite exists at deeper levels in the magmatic system and is erupted from radial dikes that apparently originate from these depths.

5.7. AN EVOLUTIONARY MODEL FOR MUSHY MAGMA CHAMBERS

On the basis of these findings, a three-stage evolutionary model for Galápagos magma chambers is proposed:

1. *The Juvenile Transient Phase (*Figure 5.6*)*: At the leading edge of the hotspot (e.g., Cerro Azul and Ecuador volcanoes), the magmatic plumbing system has

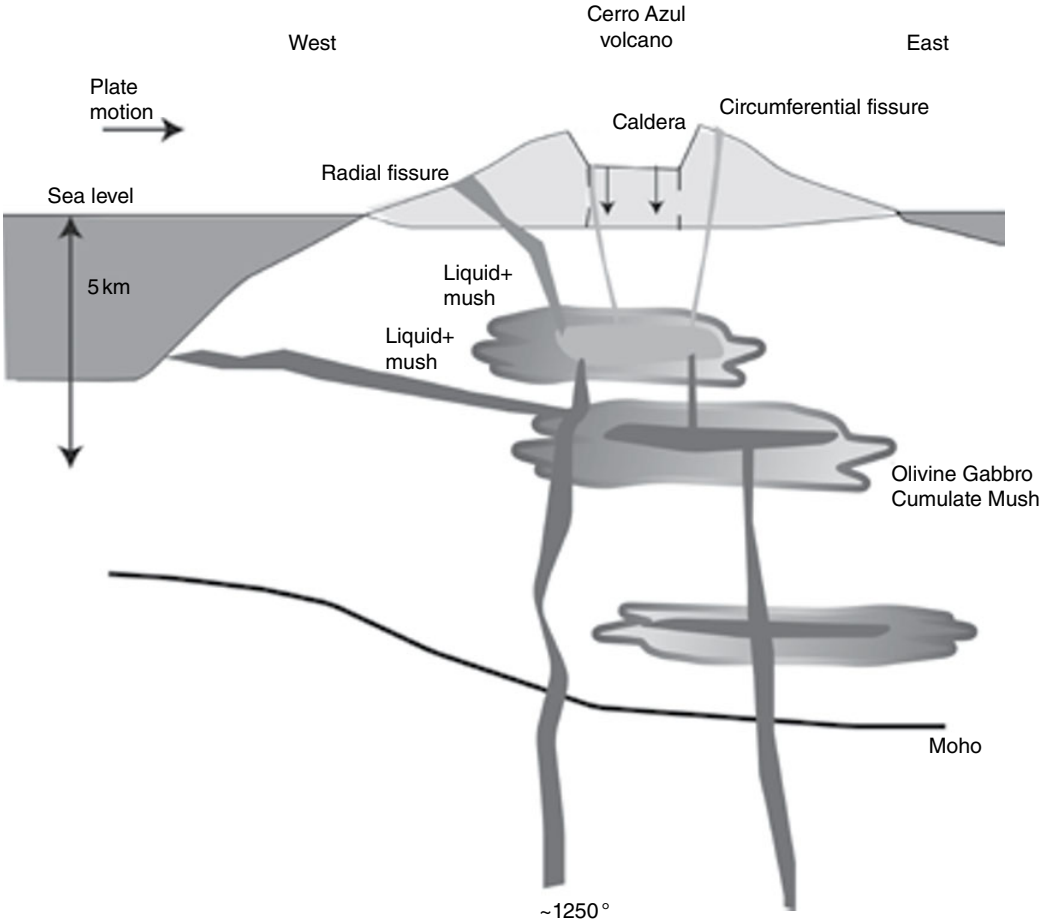

Figure 5.6 The juvenile-transient phase of volcano growth at the leading edge of the hotspot. Most of the magma reservoirs are in the lower and middle crust, and the surrounding rock is old ocean crust, although pockets of wehrlite and olivine gabbro are intersected by injected dikes. The volcano is of relatively small volume, but it has a large, deep caldera. Large temperature gradients exist in the lithosphere, and as a result, magmas evolve to varying degrees by crystallization.

yet to reach a steady state. The uppermost magma chamber tends to be deep; at Cerro Azul it is approximately 5 km deep, and there is no evidence of a shallow chamber at Ecuador [*Amelung et al*., 2000]. Different batches of magmas undergo different thermal and crystallization histories [*Naumann et al*., 2002; *Geist et al*., 2002], but they are, on average, hotter. Olivine-rich mush is flushed out of the edifice when dikes intrude and erupt [*Teasdale et al*., 2005]. The plumbing system shares many attributes of a "mush column," as proposed by *Marsh* [2005].

2. *The Mature Steady-State Phase (Figure* 5.7*)*: After a large volume of magma has crystallized within the crust and thickened it by several kilometers, the magmatic plumbing system reaches a thermal steady state, which, in the case of the monotonous volcanoes (Fernandina, Wolf, and Darwin), is about 1150 °C. Magmas undergo partial crystallization in chambers throughout the crust, and much of the crust comprises coalesced mush. The last stage of crystallization is in a thin sill about 1–3 km beneath the caldera floors (1–3 km above the regional base level). In addition to the supporting evidence of the deformation data, sills are the most stable geometry thermomechanically [*Gudmundsson*, 2012]. This sill serves as a density filter: few mafic crystals make it through the sill, but a plagioclase mush exists in the roof zone. A typical Fernandina liquid has a calculated density of 2.68 g/cm^3 at its liquidus, whereas plagioclase's density at the same conditions is 2.62 g/cm^3, and those of pyroxene and olivine are 2.78 and 3.12 g/cm^3 [*Scoates*, 2000]. Olivine-gabbro mush exists below the sill for at least 2 km (assuming that dikes do not intrude downward). At Fernandina, a deeper magma body resides at 5 km depth, and there may be magma reservoirs below that, which are undetectable by deformation at the surface.

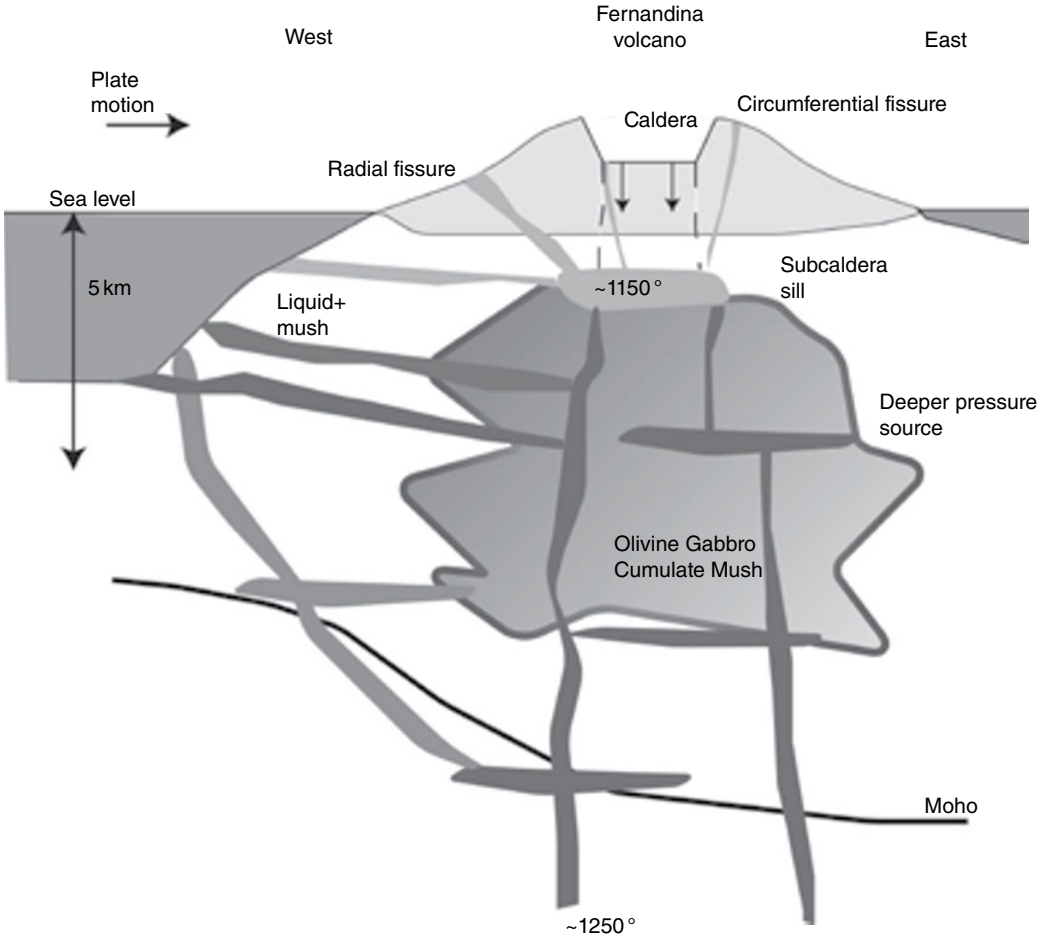

Figure 5.7 In the mature phase, the middle crust is largely composed of olivine-gabbro crystal mush, which has been deposited by magma bodies distributed throughout the crust. The uppermost chamber is a sill that lies less than 3 km beneath the caldera floor. Radially injected dikes erode the mush. The mush acts as a reactive filter [*Bedard*, 1993], buffering the magmas to constant temperature and composition. Most crustal growth occurs from above [*Lyons et al.*, 2007].

3. *The Dying Cooling Phase (Figure* 5.8*)*: As a volcano is carried away from the hotspot, the intrusive mass cools to below the previous steady-state temperature, and erupted magmas are cooler and more evolved. Alcedo volcano has erupted one of the planet's best examples of rhyolite that is produced by advanced fractional crystallization of basalt. Mass-balance indicates that the mass of mafic cumulates must be nine times that of the approximate 1 km^3 of erupted rhyolite [*Geist et al.*, 1995].

In many respects, the concept of a "magma chamber" is probably inappropriate for the Galápagos. Instead, a better concept may be a plexus of multiple intrusive bodies that are interconnected between the Moho and a shallow subcaldera sill, and magmatic evolution that is dominated by crystallization, deposition of those crystals, and subsequent reincorporation of some of those crystals. In the mature stage, the liquid magma is largely interlaced with a mafic cumulate mush, which buffers the temperature, owing to the large enthalpy of crystallization that must be removed from the system for it to cool. Thus, it is probably more appropriate to think of an integrated magmatic plumbing system rather than a dominant "magma chamber."

In most respects, this conceptual model of Galápagos magmatic plumbing systems is similar to what has been proposed for those that underlie fast-spreading mid-ocean ridges [*Sinton and Detrick*, 1992; *Boudier et al.*, 1996; *Perfit and Chadwick*, 1998], with two important differences. First, the Galápagos magmatic plumbing systems are radially symmetric; thus, the mush and liquid-rich zones are likely to be cylindrical rather than two-dimensional, making cooling more efficient in the cylindrical case. Second, there is no lithospheric spreading in the Galápagos—instead, the crust grows by thickening, although there may be lower crustal flow as well [*Jones and Maclennan*, 2005]. Ongoing seismic studies

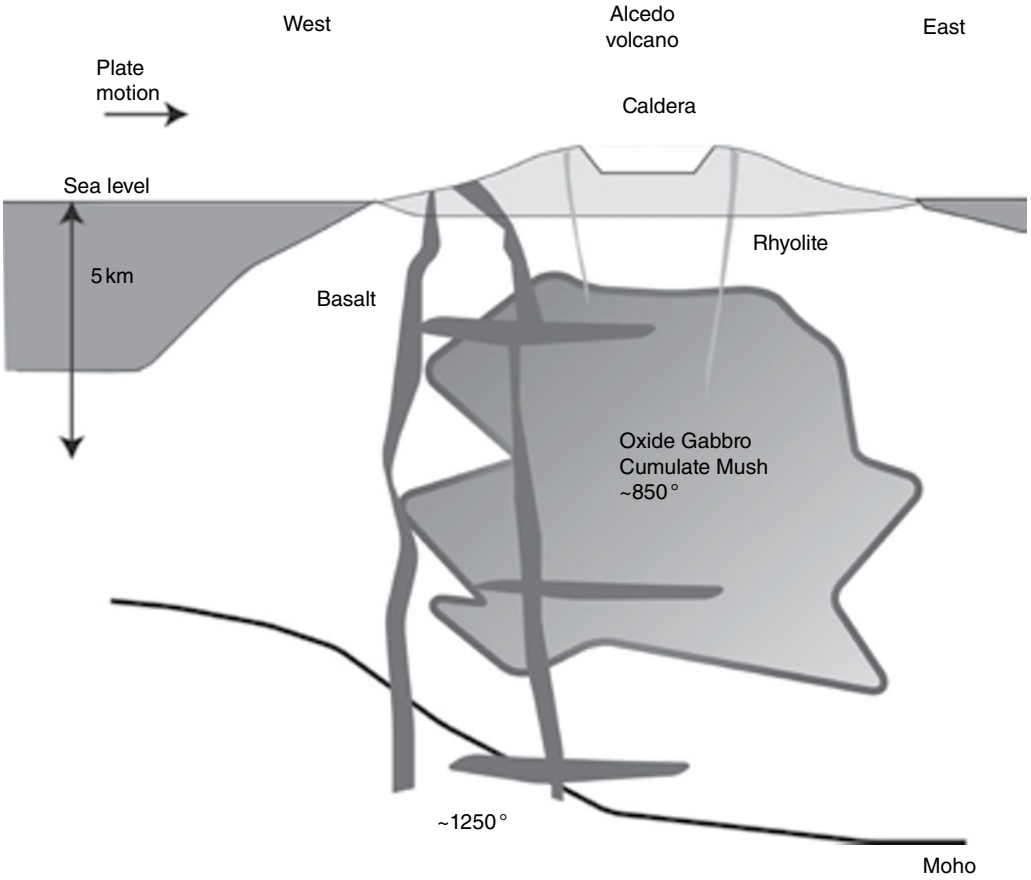

Figure 5.8 As the volcano is carried away from the hotspot, the supply of mantle-derived magma decreases, and it goes into a dying-transient phase. The crystal mush is no longer in a thermal steady state, and it begins to freeze, creating significant volumes of evolved liquid as it cools through 900°. Basaltic liquids traverse the crust with little interaction with surrounding materials.

will help reveal whether the mid and lower crust are pervasively mushy, or whether there is a series of individual sills, each surrounded by a mush zone (as proposed by *Maclennan* [2008] for Icelandic systems).

The magmatic plumbing systems feeding Galápagos volcanoes differ in important ways from those proposed for Hawaiian volcanoes, making mid-ocean ridges more appropriate analogues than the world's best-studied ocean island province. First, the mechanical behavior of Hawaiian volcanoes is dominated by rift zones, which modulate the pressurization of the shallow plumbing system and consequently the geometry of the shallow magma bodies. Second, the magma supply rate during the Hawaiian shield-building phase is almost 100 times greater than that of the Galápagos volcanoes, due to both higher productivity from the Hawaiian plume and the fact that only a few Hawaiian volcanoes are active at any one time. Third, Galápagos lavas are systematically much more evolved (and cooler) than Hawaiian tholeiites; the statistical maximum density of the Mg# of glasses from the shield-building phase of Mauna Kea [*Stolper et al.*, 2004] is 52.5, which is more primitive than any Galápagos volcano except Cerro Azul (Figure 5.4). Fourth, Galápagos magmas are multiply saturated throughout the crust [*Geist et al.*, 1998], unlike Hawaiian tholeiite, most of which is solely saturated with olivine. This has consequences for both the rheology and the chemical reactivity of the crystal mush that develops.

Despite these fundamental differences between Hawaiian and Galápagos volcanism, the evolutionary model proposed here may be analogous to changes of Hawaiian volcanism with time. During the tholeitic shield-building phase, the compositional variation of Hawaiian lavas is small: the inter-quartile range of the Mg# of Mauna Kea tholeiites (data from *Stolper et al.*, 2004] is 3.1, comparable to the dispersion of compositions from the Galápagos mature steady-state phase. In contrast, lavas erupted during the alkaline postshield phase at Mauna Kea are notably diverse, ranging from ankaramite to mugearite [*Frey et al.*, 1990], which reflect cooling and differentiation over a temperature range of hundreds of degrees. The Hawaiian postshield stage is therefore analogous to the dying cooling

phase in Galápagos, although in the former case the parental magmas intruding into the shallow system are different compositions than those of the shield-building phase.

The record from intrusive rocks does not provide much insight into the major aspects of the hypotheses put forth in this paper. Discerning any details of the supersolidus history of cumulate rocks, especially when they were in the mushy state, is notoriously difficult to determine. In terms of the density stratification of crystals proposed here, so far as we know, gabbros with excess plagioclase (beyond cotectic proportions) are not known in the upper parts of the gabbro section of the Oman ophiolite, although mafic minerals and plagioclase are density sorted on the meter to decimeter scale [*Pallister and Hopson*, 1991]. On the other hand, gabbros from the Upper Border Series of the Skaergaard Intrusion (the upper approximate 1 km of the intrusion) are richer in plagioclase than correlative rocks from the Layered Series [*Naslund*, 1984]. Likewise, thick anorthosites in the upper part of the Stillwater Complex are thought to have accumulated simultaneously with the ultramafic and mafic lower parts of the intrusion [*Meurer and Boudreau*, 1996]. We note also that lavas with plagioclase greatly in excess of cotectic or eutectic proportions are common in all tectonic environments, including elsewhere in the Galápagos [*Harpp et al.*, Chapter 15, this volume] and mid-ocean ridge basalts [*Bryan*, 1983].

5.8. CONCLUSIONS: THE DYNAMIC AND THERMAL EVOLUTION OF GALÁPAGOS MAGMA CHAMBERS

We have proposed that the compositional and petrographic variability of Galápagos lavas is attributable to temporal evolution, which exhibits transitions between crystal-poor to crystal-rich "mushy" states. These states reflect the controls that moderate- to high-crystal fraction conditions exert on magma dynamics, which can be understood in terms of three distinct stages: 1) the dilute regime, where the relative buoyancy of crystals and crystal-melt coupling dominates; 2) a mobile but crystal-rich regime where a mature and spatially continuous crystal mush buffers the intensive variables to a common temperature; and 3) a dense mush regime where the onset of crystal contiguity allows for highly evolved melts to escape and form separate magma bodies. While these magmatic stages have been recognized in arc and mid-ocean ridge systems, they are expressed especially well in the Galápagos, allowing one to understand them as a continuum of multiphase processes.

The dilute stage refers to conditions where the volumetric proportion of crystals is much lower than that of the melt phase, and the coupling in the dynamics is largely due to the movement of the melt phase acting on individual crystals. The threshold of the volume fraction of solids where dilute conditions no longer apply is not well defined [*Burgisser and Bergantz*, 2002; *Burgisser et al.*, 2005], but the fundamental physical processes can still be described. Of primary interest is the way that the motion of the melt can control the distribution and mixing of the crystals. The crystals will experience a steady acceleration from gravity and an unsteady acceleration from the fluid motion. Because these two forces are not the same in time, the resulting velocities cannot simply be added to obtain the crystal travel path.

The importance of buoyancy for settling compared to crystal transport by the fluid can be expressed with the dimensionless gravitational settling number:

$$G_T = \frac{\rho_p g d^2}{18 f \mu \Delta U}$$

Where ρ_p is the particle density, g is the scalar acceleration of gravity, d is the crystal diameter, f is the drag factor, μ is the dynamic viscosity and ΔU is the characteristic fluid velocity. If this ratio is much greater than one, crystal sedimentation dominates, and if less than one transport of the crystals by convection of the melt dominates and sedimentation will be restricted to the boundary layer at the bottom of the magma chamber.

A second, non-steady form of coupling between crystals and melt arises from the way that crystals respond to the forces of the fluid. This is not related to gravity, but instead is the response of a crystal to the melt motion. At one end, the crystals will act as tracers and follow the melt velocity field perfectly, and at the other end, they will not respond to the fluid-forcing at all and be perfect ballistic particles. This behavior can be expressed with a ratio called the Stokes number:

$$S_T = \frac{\Delta\rho d^2 \Delta U}{18 f \mu \delta}$$

where $\Delta\rho$ is the density contrast between crystals and melt, d is the crystal diameter, ΔU is the characteristic fluid velocity, f is the drag factor, μ is the dynamic viscosity, and δ is the characteristic distance or eddy diameter of the fluid flow. If the Stokes number is much less than unity, the crystals are perfect tracers, and if the Stokes number is much greater than unity, the crystals will not be influenced by the melt convection. If the Stokes number is about unity, the crystals will migrate to the margins of eddies and self-organize there [*Crowe et al.*, 1985].

End-member combinations of the gravitational settling number and the Stokes number will produce distinct regimes that can be recognized in the magmatic products [*Burgisser et al.*, 2005]. If both the Stokes and gravitational settling number are less than unity, the system can be described as being well-mixed as long as the magmatic convection is chaotic. Crystals are entrained by the rapid

convection and the formation of eddies, and the vigor of the melt phase dictates the location and degree of mixing. These conditions are most likely to arise when intrusion of crystal-poor magmas form new chambers with large surface area and undergo rapid cooling and convection [*Marsh*, 1989], producing locally well-mixed mobile bodies. Since the vigor of the melt convection is not likely to be uniform in space and time, diverse compositions can emerge from the continued entrainment of the crystal cargo with the melt convection, reflecting different combinations of the Stokes and gravitational settling numbers. Even if the Stokes number is less than unity, rather small differences in the Stokes number of crystals of different type—say olivine and pyroxene—can lead to subtle local variability in the mode that will be expressed in compositional variation, even in a system that is still being actively stirred.

As cooling proceeds and crystallinity increases, the vigor of convection will diminish. This is due to the decrease in heat flux through the margins if there are solidification fronts, the thermal loading from the conjugate heat transfer at the margins [*Bergantz*, 1992; *Bergantz and Lowell*, 1987], and the increase in bulk viscosity from the presence of crystals. These conditions motivate the end-member where both the Stokes and gravitational settling numbers are much greater than unity. In this case, crystal segregation can occur by hindered settling and flotation [*Marsh*, 1988]. In a multiply saturated Galápagos magma, this would produce an "unmixed" layered system with the olivine and pyroxene sinking and the plagioclase floating. This combination of Stokes and gravitational-settling numbers is likely to be the case within the shallow sill in mature Galápagos systems.

Our interpretation of monotonous Galápagos magmatic systems is that the crystal-rich volume is significantly larger than the volume of new magma injection. New injections intrude into and mix with the existing crystal mush. The details of this process are not well understood, but the buffering to a common magmatic temperature over millenia indicates that the mush body is sufficiently large to "clamp" the system to a common environment of fixed intensive variables. An important corollary to this is that the mush is still mobile—enough to allow for mixing, reequilibration, and continued phase separation such that submarine flank eruptions are dominantly olivine and pyroxene and subaerial eruptions dominantly plagioclase. Importantly, we interpret most crystals in Galápagos lavas as antecrysts, as they did not initially form in the melts within which they were erupted. The physics of the process of new intrusions disrupting and reequilibrating with a resident large crystal slurry is not well understood, and existing models rely on parameterizations with highly simplified rheological relationships [*Burgisser and Bergantz*, 2011].

As magmatic systems move away from the hotspot, continued cooling produces an increase in crystallinity such that contiguity, a condition of crystal "lock up," can occur. This allows for the relative motion of evolved interstitial melt by a number of poorly understood processes such as (but not limited to) micro-settling, compaction, gas sparging, and mush fracture *[Bachmann and Bergantz*, 2004, 2006, 2008a,b]. The existence of small volumes of siliceous rocks in the archipelago suggests that simple tearing of plastic mush or an in-situ process like compaction is insufficient to produce volumetrically significant, evolved magmas from the subjacent mafic crystal mush. This raises the interesting question: are evolved melts more common but generally uneruptable, or are special conditions necessary for their segregation and eruption?

5.9. ACKNOWLEDGMENTS

The authors are grateful to the National Science Foundation for funding this work (grants EAR-0838461 and EAR-1145271 to Geist, EAR-0809574 and EAR-0930045 to Chadwick, and EAR 1049886 and EAR 0711551 to Bergantz) and providing assistance for the Chapman Conference (EAR 1014620). This work could not have been completed without the logistical support of the Charles Darwin Research Station and the Galápagos National Park. Much of the real work that enabled this paper was accomplished by Bob Reynolds, Terry Naumann, Rachel Teasdale, Bridget Diefenbach, Ellen Hedfield, and John Lyons while they were graduate students at the University of Idaho. John Maclennan suggested the statistical tools used to generate Figure 5.4. We thank him, Marco Bagnardi, and Falk Amelung for their constructive reviews and Karen Harpp for her editorial help. PMEL contribution number 3863.

REFERENCES

Albarède, F. (1993), Residence time analysis of geochemical fluctuations in volcanic series. *Geochim. Cosmochim. Acta*, *57*, 615–621.

Allan, J.F. and T. Simkin (2000), Fernandina Volcano's evolved, well-mixed basalts: Mineralogical and petrological constraints on the nature of the Galápagos plume, *J. Geophys. Res.*, *105*, 6017–6031.

Amelung, F., S. Jónsson, H. Zebker, and P. Segall (2000), Widespread uplift and "trapdoor" faulting on Galápagos volcanoes observed with radar interferometry, *Nature*, *407*, 993–998.

Argus, D. F. et al. (2010), The angular velocities of the plates and the velocity of Earth's centre from space geodesy. *Geophys. J. Int*, *180*, 913–960. doi: 10.1111/j.1365-246X.2009.04463.x

Bachmann, O., and G.W. Bergantz (2004), On the origin of crystal-poor rhyolites: Extracted from batholithic crystal mushes, *J. Petrol.*, *45*, 1565–1582.

Bachmann, O., and G.W. Bergantz (2006), Gas percolation in upper-crustal silicic crystal mushes as a mechanism for upward heat advection and rejuvenation of near-solidus magma bodies, *J. Volc. Geothermal Res.*, *149*, 85–102.

Bachmann, O., and G.W. Bergantz (2008a), The magma reservoirs that feed supereruptions, *Elements*, *4*, 17–21.

Bachmann, O., and G.W. Bergantz (2008b), Rhyolites and their source mushes across tectonic settings, *J. Petrol.*, *49*, 2277–2285.

Bagnardi, M., and F. Amelung (2012), Space-geodetic evidence for multiple magma reservoirs and subvolcanic lateral intrusions at Fernandina Volcano, Galápagos Islands. *J. Geophys. Res.*, 117, DOI: 10.1029/2012JB009465.

Bergantz, G.W. (1992), Conjugate solidification and melting in multicomponent open and closed systems,. *Int. J Heat Mass Transfer*, *35*, 533–543.

Bergantz, G.W. (1995), Changing techniques and paradigms for the evaluation of magmatic processes, *J. Geophys Res*, *100*, 17603–17613.

Bergantz, G.W., and R.P. Lowell (1987), The role of conjugate convection in magmatic heat and mass transfer, in Structure and Dynamics of Partially Solidified Systems: NATO ASI Series, Series E, No. 125 edited by D.E. Loper: Dordrecht, Martinus Nijhoff, 367–382.

Boudier, F., A. Nicolas, and B. Ildefonse (1996), Magma chambers in the Oman ophiolite: fed from the top and the bottom, *Ear. Planet. Sci. Lett.*, *144*, 239–250.

Burgisser, A., and G.W. Bergantz (2002), Reconciling pyroclastic flow and surge: the multiphase physics of pyroclastic density currents, *Earth Plan. Sci. Lett.*, *202*, 405–418.

Burgisser, A., and G.W. Bergantz (2011), A rapid mechanism to remobilize and homogenize highly crystalline magma bodies, *Nature*, *471*, 212–215.

Burgisser, A., G.W. Bergantz, and R.E. Breidenthal (2005), Addressing complexity in laboratory experiments: the scaling of dilute multiphase flows in magmatic systems, *J. Volc. Geothermal Res.*, *141*, 245–265.

Bedard, J.H. (1993), Oceanic crust as a reactive filter; synkinematic intrusion, hybridization, and assimilation in an ophiolitic magma chamber, western Newfoundland, *Geology*, *21*, 77–80.

Bryan, W.B. (1983), Systematics of modal phenocryst assemblages in submarine basalts: Petrologic implications, *Contrib. Mineral. Petrol.*, *83*, 62–74.

Chadwick, W.W., Jr. and K.A. Howard (1991), The pattern of circumferential and radial eruptive fissures on the volcanoes of Fernandina and Isabela islands, Galápagos, *Bull. Volcanol.*, *53*, 259–275.

Chadwick, W.W., Jr., T. De Roy, and A. Carrasco (1991), The September 1988 intra-caldera avalanche and eruption at Fernandina volcano, Galápagos Islands, *Bull. Volcanol.*, *53*, 276–286.

Chadwick, W.W., Jr., and J.H. Dieterich (1995), Mechanical modeling of circumferential and radial dike intrusion on Galápagos volcanoes, *J. Volcanol. Geotherm. Res.*, *66*, 37–52.

Chadwick, W.W., Jr. et al. (2006), A volcano bursting at the seams: Inflation, faulting, and eruption at Sierra Negra Volcano, *Galápagos, Geology*, *34*, 1025–1028.

Chadwick, W.W., Jr. et al. (2011), The May 2005 eruption of Fernandina volcano, Galápagos: The first circumferential dike intrusion observed by GPS and InSAR, *Bull. Volcanol.*, *73*, 679–697.

Crowe, C.T., R.A. Gore, and T.R. Troutt (1985), Particle dispersion in free shear flows, *Part. Sci. Tech.*, *3*, 149–158.

Filson, J., T. Simkin, and L.K. Leu (1973), Seismicity of a caldera collapse: Galápagos Islands 1968, *J. Geophys. Res.*, *78*, 8591–8622.

Frey, F.A. et al. (1990), Evolution of Mauna Kea Volcano, Hawaii: Petrologic and geochemical constraints on postshield volcanism, *J. Geophys. Res.*, *95*, 1271–1300, doi:10.1029/JB095iB02p01271.

Geist, D., K.A. Howard, A.M. Jellinek, and S. Rayder (1994), The volcanic history of Volcan Alcedo, Galápagos Archipelago: A case study of rhyolitic oceanic volcanism, *Bull. Volcanol.*, *86*, 243–260.

Geist, D., K.A. Howard, and P.B. Larson (1995), The generation of oceanic rhyolites by crystal fractionation: The basalt-rhyolite association at Volcan Alcedo, Galápagos Archipelago, *J. Petrol.*, *36*, 965–982.

Geist, D.J., T.R. Naumann and P.L. Larson (1998), Evolution of Galápagos magmas: mantle and crustal fractionation without assimilation, *J. Petrol.*, *39*, 953–971.

Geist, D. et al. (2002), Volcanic evolution in the Galápagos: The dissected shield of Volcan Ecuador, *Geochem. Geophys., Geosys.*, *3*, doi:10.1029/2002GC000355.

Geist, D. et al. (2005), Wolf Volcano, Galápagos Archipelago Melting at the margins of a plume and a model for magmatic evolution, *J. Petrol. 46*, 2197–2224.

Geist, D., W.W. Chadwick, and D.J. Johnson (2006a), Results from new GPS and gravity monitoring networks at Fernandina and Sierra Negra Volcanoes, Galápagos, 2000–2002, *J. Volcanol. Geotherm. Res.*, *150*, 79–97.

Geist, D. et al. (2006b), Submarine Fernandina: A magmatic plumbing system at the leading edge of the Galápagos Hotspot, *Geochem. Geophys., Geosys.*, *7*, DOI 10.1029/2006GC001290.

Geist, D. et al. (2008a), Construction of the Galápagos platform by large submarine volcanic terraces, *Geochem. Geophys., Geosys.*, *9*, doi:10.1029/2007GC001795.

Geist, D.J. et al. (2008b), The 2005 eruption of Sierra Negra volcano, Galápagos, Ecuador, *Bull. Volcanol. 70*, 655–673.

Ghiorso, M.S., and R.O. Sack (1995), Chemical mass transfer in magmatic processes IV: a revised and internally consistent thermodynamic model for the interpolation and extrapolation of liquid-solid equilibria in magmatic systems at elevated temperatures and pressures, *Contrib. Mineral. Petrol.*, *119*, 197–212.

Gudmundsson, A. (2012), Magma chambers: Formation, local stresses, excess pressures, and compartments, *J. Volcanol. Geotherm. Res.*, *237–238*, 19–41.

Harpp, K.S. et al. (2014), Plume-ridge interaction in the Galápagos: Perspectives from Wolf, Darwin, and Genovesa Islands, Chapter 15, this volume.

Hedfield, E. (2003), Insight into the magmatic evolution of Fernandina volcano, Galápagos, from olivine- and plagioclase-hosted melt inclusions, unpublished M.S. thesis, University of Idaho, Moscow, ID USA.

Howard, K.A. (2010), Caldera collapse: Perspectives from comparing Galápagos volcanoes, nuclear-test sinks, sandbox models, and volcanoes on Mars, *GSA Today*, *20*(10), 4–10.

Huppert, H.E., R.S.J. Sparks, J.A. Whitehead, and M.A. Hallworth (1986), Replenishment of magma chambers by light inputs, *J. Geophys. Res*, *91*, 6113–6122.

Huppert, H.E. and R.S.J. Sparks (1988), The Generation of Granitic Magmas by Intrusion of Basalt into Continental Crust, *J. Petrology 2*, 599–624.

Jones, S.M., and J. Maclennan (2005), Crustal flow beneath Iceland, *J. Geophys. Res.*, *110*, B09410, doi:10.1029/2004JB003592.

Jónsson, S. (2009), Stress interaction between magma accumulation and trapdoor faulting on Sierra Negra Volcano, Galápagos, *Tectonophysics*, *471*(1–2), 36–44.

Jónsson, S., H. Zebker, and F. Amelung (2005), On trapdoor faulting at Sierra Negra volcano, Galápagos, *J. Volcanol. Geotherm. Res.*, *144*, 59–71.

Kelemen, P.B., K. Koga, and N. Shimizu (1997), Geochemistry of gabbro sills in the crust- mantle transition zone of the Oman ophiolite: Implications for the origin of the oceanic lower crust, *Earth Planet. Sci. Lett.146*, 475–488.

Koleszar, A.M. et al. (2009), The volatile contents of the Galápagos plume; evidence for H2O and F open system behavior in melt inclusions, *Earth Planet. Sci. Lett. 287*, 442–452.

Kurz, M.D., S. Rowland, J. Curtice, A. Saal, and T. Naumann (2014), Eruption rates for Fernandina volcano: a new chronology at the Galápagos hotspot center, Chapter 4, this volume.

Lyons, J. et al. (2007), Crustal growth by magmatic overplating in the Galápagos, *Geology*, *35*, 511–514.

Maclennan, J. (2008), Concurrent Mixing and Cooling of Melts under Iceland, *J. Petrology*, *49*, 1931–1953, doi:10.1093/petrology/egn052.

Maclennan, J., T. Hulme, and S.C. Singh (2004), Thermal models of oceanic crustal accretion: Linking geophysical, geological and petrological observations, *Geochem. Geophys. Geosyst.*, *5*, Q02F25, doi:10.1029/2003GC000605.

Marsh, B.D. (1988), Crystal capture, sorting and retention in convecting magma, *Geol. Soc. Amer. Bull.*, *100*, 1720–1737.

Marsh, B.D. (1989), Magma chambers, *Ann. Rev. Earth. Planet Sci.*, *15*, 439–74.

Marsh, B.D. (1989), On convective style and vigor in sheet-like magma bodies, *J. Petrology*, *30*, 479–530.

Marsh, B. (2005), A magmatic mush column Rosetta Stone; the McMurdo dry valleys of Antarctica, *Eos. Trans. Amer. Geophys. Union*, *85*, 497–502.

McBirney, A.R. (1980), Mixing and unmixing of magmas, *J. Volcanol. Geotherm. Res. 7*, 357–371.

McBirney, A.R. and H. Williams (1969), Geology and petrology of the Galápagos Islands. *Geolog. Soc. Amer. Mem.*, *118*, 197.

Mouginis-Mark, P.J., S.K. Rowland, and H. Garbeil (1996), Slopes of western Galápagos volcanoes from airborne interferometric radar, *Geophys. Res. Lett.*, *23* (25), 3767–3770.

Meurer, W.P., and A.E. Boudreau (1996), Petrology and mineral compositions of the middle banded series of the Stillwater Complex, *Montana. J. Petrol.*, *37*, 583–607.

Munro, D.C. and S.K. Rowland (1996), Caldera morphology in the western Galápagos and implications for volcano eruptive behavior and mechanisms of caldera formation. *J. Volcanol. Geotherm. Res. 72*, 85–100.

Naslund, H.R. (1984), Petrology of the Upper Border Series of the Skaergaard Intrusion, *J. Petrology 25*, 185–212 doi:10.1093/petrology/25.1.185

Naumann, T., and D. Geist (2000), Physical volcanology and structural development of Cerro Azul volcano, Isabela island, Galápagos: Implications for the development of Galápagos-type shield volcanoes, *Bull. Volcanol.*, *61*, 497–514.

Naumann, T.R., D. Geist, and M.D. Kurz (2002), Petrology and geochemistry of Volcan Cerro Azul: petrologic diversity among the western Galápagos volcanoes, *J. Petrol.*, *43*, 859–883.

Naumann, T.R. and L. Krebs (2003), Petrology and Geochemistry of Volcan Darwin, Isabela Island, Galápagos Archipelago. American Geophysical Union, Fall Meeting, abstract #V12D-0618.

Nordlie, B.E. (1973), Morphology and structure of the western Galápagos volcanoes and a model for their origin, *Geol. Soc. Am. Bull.*, *84*, 2931–2956.

Pallister, J.S., and C.A. Hopson (1981), Semail ophiolite plutonic suite: Field relations, phase variation, cryptic variation and layering, and a model of a spreading ridge magma chamber, *J. Geophys. Res. 86*, 2593–2644.

Perfit, M.R., and W.W. Chadwick, Jr. (1998), Magmatism at mid-ocean ridges: Constraints from volcanological and geochemical investigations, in Faulting and Magmatism at Mid-Ocean Ridges, *Geophys. Monograph 106*, ed. W. R. Buck, et al., 59–116.

Reynolds, R., D. Geist, and M. Kurz (1995), Physical volcanology and structural development of Sierra Negra volcano, Galápagos Archipelago, *Geol. Soc. Am. Bull. 107*, 1398–1410.

Rowland, S.K., and D.C. Munro (1992), The caldera of Volcan Fernandina: A remote sensing study of its structure and recent activity, *Bull. Volcanol.*, *55*(1–2), 97–109

Ryan, W.B.F. et al. (2009), Global Multi-Resolution Topography synthesis, *Geochem. Geophys. Geosyst.*, *10*, Q03014, doi:10.1029/2008GC002332.

Ryland, S.L. (1971), A gravity and magnetic study of the Galápagos Islands, M.S. thesis, University of Missouri, Columbia, MO USA, *57*.

Scoates, J.S. (2000), The plagioclase–magma density paradox re-examined and the crystallization of Proterozoic anorthosites, *J. Petrology*, *41*, 627–649. doi:10.1093/petrology/41.5.627.

Simkin, T. (1972), Origin of some flat topped volcanoes and guyots, *Geol. Soc. Amer. Mem.*, *132*, 183–193.

Simkin, T. and L. Siebert (1994), Volcanoes of the World, 2nd ed. Tucson, AZ: Geoscience Press, 349.

Simkin, T., and K.A. Howard (1970), Caldera collapse in the Galápagos Islands, 1968, *Science*, *169*, 429–437.

Sinton, J.M., and R.S. Detrick (1992), Mid-ocean ridge magma chambers, *J. Geophys. Res.*, *97*, 197–216.

Stolper, E., S. Sherman, M. Garcia, M. Baker, and C. Seaman (2004), Glass in the submarine section of the HSDP2 drill core, Hilo, Hawaii, *Geochem. Geophys. Geosyst.*, *5*, Q07G15, doi:10.1029/2003GC000553.

Teasdale, R., D. Geist, M. Kurz, and K. Harpp (2005), 1998 Eruption at Volcan Cerro Azul, Galápagos Islands: I. Syn-Eruptive Petrogenesis, *Bull. Volcanol.*, *67*, 170–185.

Vigouroux, N. et al. (2008), 4D gravity changes associated with the 2005 eruption of Sierra Negra volcano, *Galápagos, Geophysics*, *73*, WA29–WA35.

Walker, G.P. (1988), Three Hawaiian calderas: An origin through loading by shallow intrusions? *J. Geophys. Res.*, *93*, 14773–14.

Wessa, P. (2013), Free Statistics Software, Office for Research Development and Education, version 1.1.23-r7, URL http://www.wessa.net/.

Yun, S.–H., P. Segall, and H.A. Zebker (2006), Constraints on Magma Chamber Geometry at Sierra Negra Volcano, Galápagos Islands, based on InSAR Observations, *J. Volcanol. Geotherm. Res.*, *150*, 232–243.